Research Article

Hawdang Othman Abdalla, Martyna Warzańska, Jakub Grajewski, and Radosław Mrówczyński*

Chirality and self-assembly of structures derived from optically active 1,2-diaminocyclohexane and catecholamines

https://doi.org/10.1515/ntrev-2024-0090 received May 2, 2024; accepted August 1, 2024

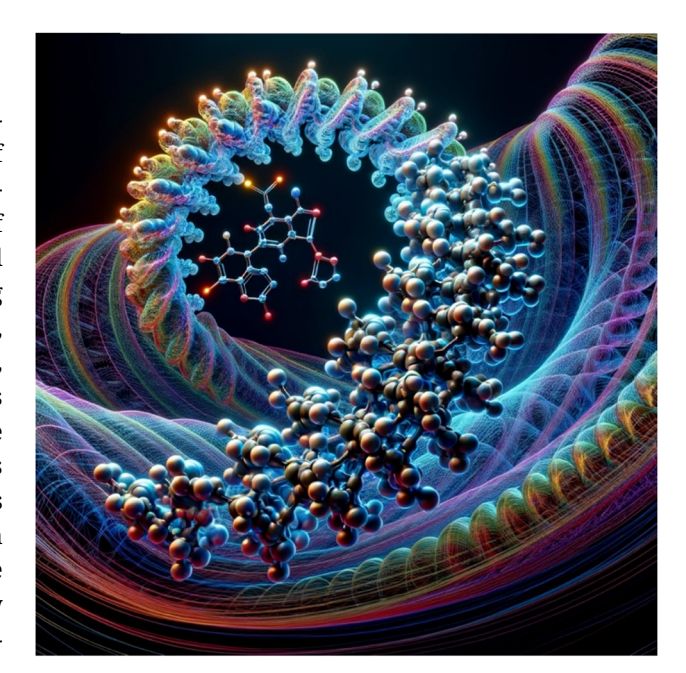
Abstract: Chiral biomimetic nanostructures were successfully synthesized through the oxidative polymerization of chiral and achiral catecholamines in the presence of optically active 1,2-diaminocyclohexane (DACH). Analysis of these nanostructures using circular dichroism confirmed their chiral nature, demonstrating the feasibility of inducing chirality in achiral polycatecholamine materials. Furthermore, the chiral nanostructures exhibited self-assembly behaviour, forming distinctive patterns or curly carpets-like structures on silicon surfaces. The arrangement and morphology of these structures were closely linked to the amount of DACH and its inherent chirality. Additionally, the self-assembly process was shown to be significantly influenced by the pH of the reaction and the choice of supporting materials. These findings are particularly relevant in the context of molecular self-assembly of nanoaggregates/particles generated during dopamine polymerization, suggesting a promising avenue for the development of novel chiral polycatechols-based materials.

Keywords: chiral nanomaterials, polydopamine, catechol, chirality, DACH

1 Introduction

Among the diverse range of molecules applied in organic synthesis and material chemistry, 1,2-diaminocyclohexane (DACH) has garnered significant attention from the scientific

Hawdang Othman Abdalla, Martyna Warzańska, Jakub Grajewski: Faculty of Chemistry, Adam Mickiewicz University, Uniwersytetu Poznańskiego 8, 61-614 Poznań, Poland



Graphical abstract

community. This optically active diamine has been utilized in the synthesis of chiral ligands that have demonstrated broad applications in organocatalytic asymmetric reactions and chiral recognition [1-3]. Additionally, DACH has found use in the synthesis of a novel class of macrocycles, termed trianglimines, which are produced from selected aromatic dialdehydes [4,5]. The DACH molecules have additionally found application in the synthesis of molecular cages, gigantocycles and perovskite, thus demonstrating the extensive versatility of this chiral building block [6,7]. Furthermore, the DACH also creates a backbone for the molecules that are used as organocatalysts and chiral auxiliary as well as intriguing chiral photoactive materials [8]. It has also been shown that DACH macrocycles-based sorbents exhibit remarkable moisture sorption properties. In this report, it has been proved that the hydration state of the trianglimines crystal can be visualized over a wide temperature range, making it an important tool for studying the dynamics of water molecules in materials [9].

^{*} Corresponding author: Radosław Mrówczyński, Faculty of Chemistry, Adam Mickiewicz University, Uniwersytetu Poznańskiego 8, 61-614 Poznań, Poland; Center for Advanced Technologies, Adam Mickiewicz University, Uniwersytetu Poznańskiego 10, 61-614 Poznań, Poland, e-mail: radoslaw.mrowczynski@amu.edu.pl

Polycatecholamines have garnered significant attention from scientific communities due to their biocompatibility and straightforward preparation methods, which enable the production of nanoparticles and coatings on various substrates with different chemical characteristics [10-14]. One of the most well-known and versatile materials belonging to this group is polydopamine (PDA) [15-20]. This black biomimetic polymer with strong adhesive properties is synthesized through oxidative polymerization of dopamine in basic conditions. Although the PDA structure is still somewhat elusive, the literature suggests that it consists of an indole ring connected via aromatic carbon atoms and may contain free, open ethylamino chains [21]. Furthermore, the presence of quinone groups allowed its functionalization with amines and thiols. Lately, the scope of PDA functionalization has been extended to azide rendering it capable for click chemistry [22,23]. In order to obtain modified PDA coatings, scientists have developed a promising strategy that involves adding various amine-bearing molecules to dopamine polymerization reactions [24,25]. This approach has been extended by different groups which, added branched polyethyleneimine with different molecular weights to dopamine polymerization reactions, resulting in the production of a novel coating material that can be applied in various applications [26–28]. The precise control of dopamine polymerization reactions has led to the development of PDA nanomaterials, which are versatile and multifunctional nanoplatforms for combined oncological therapies [29-31]. Moreover, the use of naturally occurring catecholamines such as chiral L-DOPA and norepinephrine has enabled the preparation of new coatings and particles for different applications, including material chemistry and medicine [32-35].

Chiral nanomaterials have come under considerable attention across various scientific disciplines, distinguished by their unique properties that have broad implications in fields ranging from catalysis to medicine [36-40]. The domain of inorganic chiral nanoparticles, particularly those based on gold, silica, or cobalt oxide, has seen rapid development due to their promising applications. Recent contributions by Prato and colleagues in synthesizing chiral carbon quantum dots have expanded the repertoire of chiral nanomaterials [41,42] showcasing properties that could revolutionize sensor technology, drug delivery, and beyond. Similarly, the Kumar group has pioneered the use of natural chiral compounds like glutathione and citric acid as starting materials for chiral carbon nanostructures, further bridging the gap between organic chemistry and nanotechnology [43]. The Rogach group's extensive research on transferring chirality from biologically-derived compounds to carbon nanomaterials have set a precedent for the synthesis of chiral structures with enhanced functionality.

Despite these advancements, the exploration of chiral nanoparticles in the realm of polymeric and soft materials remains relatively nascent. A notable exception is the work by Awasthi *et al.*, who reported the synthesis of chiral PDA nanoribbons using phenylalanine-based amphiphiles as soft templates [44]. This innovative approach underscores the potential of leveraging biomolecules for the directed synthesis of chiral polymeric materials. However, the synthesis of chiral polymeric polycatecholamine nanomaterials, particularly through the induction of chirality from a dopant to the resultant polycatechol structures, is yet to be reported. This uncharted territory represents fertile ground for breakthroughs in the development of new, innovative chiral nanomaterials.

Here we describe a new approach for the synthesis of chiral polycatecholamines nanostructures, a frontier yet to be fully explored in chiral nanomaterials research. By integrating a chiral molecule - DACH into the molecular architecture during the polymerization of catecholamines such as dopamine, L-DOPA, and D/L-norepinephrine under basic conditions – we have unlocked a new class of materials. These chiral polycatecholamines not only embody the inherent biocompatibility and versatility of their base compounds but also introduce a novel chiral dimension that significantly influences their self-assembly and surface interaction properties. A hallmark of our findings is the discovery of unique patterns formed on silicon wafers through the self-assembly of these chiral polycatecholamines. This morphological innovation contrasts sharply with the traditional patterns observed in PDA and related materials synthesis, underscoring the pivotal role of chiral DACH in directing the self-assembly process. Thus, our work not only contributes a novel material to the chiral nanomaterials landscape but also addresses a significant research gap by demonstrating the feasibility of inducing chirality in PDA and related polymers through the dopant's molecular architecture. This approach signifies a step forward in the rational design and synthesis of chiral materials, offering a replicable strategy for researchers seeking to infuse chirality into other polymeric systems both macro and nanoscale.

2 Methods

2.1 Materials

Dopamine hydrochloride was purchased from Alfa Aesar. L-DOPA was purchased from Ambeed, D/L-norepinephrine and TRIZMA base were provided by Merck Life Sciences. In all reactions, the MiliQ water was used characterized by resistivity of 18.2 M Ω cm at 25°C.

2.2 Nanoparticles characterization

The TEM images of obtained materials were obtained using the Transmission Electron Microscope JEM-1400 (JEOL, Japan). To prepare a sample, a drop of the reaction mixture of particles in water was added on a Lacey Formvar/ Carbon grid (300 mesh, Copper approx. grid hole size: 63 µm) and left to dry overnight. Both dynamic light scattering (DLS) and zeta potential were recorded using Zeta Malvern Zetasizer Nano ZS. The morphology of the materials was imaged by scanning electron microscopy (SEM) Quanta 250 FEG, FEI. The circular dichroism (CD)/UV-VIS measurements were performed on JASCO J-810 (JASCO, Tokyo, Japan) at ambient temperature. Spectra were recorded in the range of 190-400 nm in TRIS solutions at 200 nm/min, with data pitch of 0.5 nm with 6 accumulations to keep the noise at the acceptable level. The measurements were made in an N₂ flow (15 L/min) at the optical path length of 1.0 mm. Samples were measured after synthesis without additional dilution (concentrations were the same for all solutions). Due to the nature of the obtained oligomers, UV spectra are a composite of the absorption of the analysed compounds and their dispersion in solution.

2.3 General protocol for reaction polymerization of catecholamine in the presence of DACH

In a 25 cm³ round bottom flask, 2 mL of DACH stock solution (12 mg in 10 mL of TRIS buffer, 10 mmol, pH = 9) was added, followed by the addition of dopamine hydrochloride (2 mg) in TRIS buffer (10 mmol, pH = 9, 1 mL). The final volume of the reaction was adjusted to 10 mL. The reaction was stirred exposed to air at a speed of 100 rpm. After 24 h, the crude reaction mixture was centrifuged at 12,400 rpm for 10 min. The obtained particles were collected, washed once with water, and then redispersed in fresh water. The molar ratio between dopamine and DACH was controlled by changing the volume of DACH from the stock solution. In order to prepare SEM samples, a supernatant of 20 µL obtained from the reactions between DACH and dopamine was drop casted onto a silicon wafer. This solution was then allowed to evaporate under ambient temperature. The same procedure was applied to the obtained particles respired in water. It is worth emphasizing that the phenomenon of dopamine polymerization in the presence of DACH results in the formation of two distinct fractions. One comprises solid particles present in relatively small quantities that can be effectively isolated. The other type is comprised of small aggregates or oligomers that remain in solution. In the case of dopamine, both material fractions were investigated by SEM. In the case of L-DOPA, we did not observe precipitation of particles; therefore, we drop casted the raw mixture on a silicon wafer. For D/L-norepinephrine, only a very small amount of particles could be centrifuged and separated from the supernatant before drop casting on a silicon support.

2.4 Influence of the pH and support on the self-assembly process

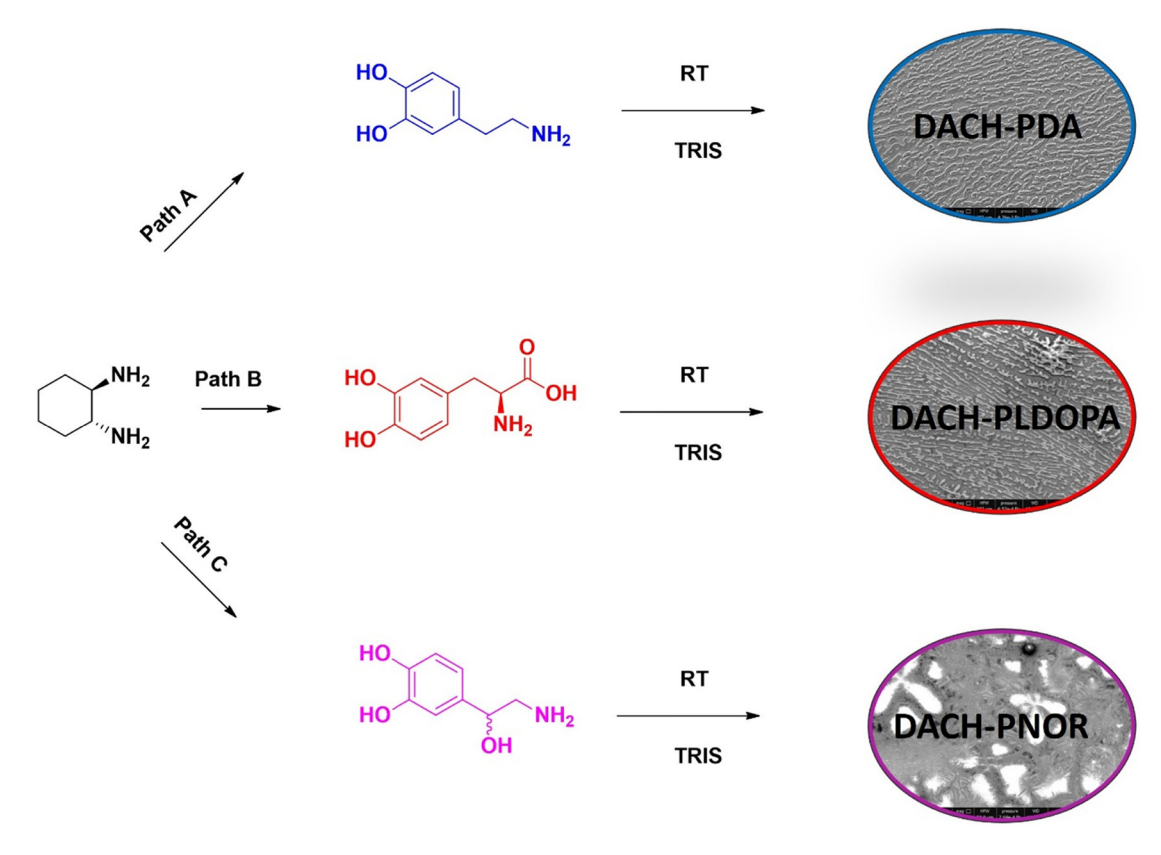
To investigate the impact of pH on the self-assembly process of particles generated through the reaction between dopamine and DACH on silicon support, we conducted a series of experiments wherein we varied the pH of the TRIS buffer from 7.5 to 9.5 with a step change of 0.5 in the pH value. Additionally, we explored the effect of support on the self-assembly of the same particles by substituting the silicon wafer with a glass slide and aluminium foil.

3 Results and discussion

The schematic representation of the polymerization of catecholamines in the presence of DACH is illustrated in Scheme 1.

3.1 Approach A – reaction between (R,R)-**DACH** and dopamine

In our preliminary exploration of chiral polycatecholamines, we embarked on the polymerization of dopamine, which is devoid of stereogenic centres and thus, inherently achiral. The polymerization was facilitated in the presence of the chiral catalyst (R,R)-DACH, which is characterized by two amino groups tethered to a six-membered aliphatic ring. The polymerization process was conducted within a TRIS buffer solution, maintaining a pH of 9 and a dopamine concentration of 1×10^{-3} mol. To assess the influence of (R,R)-DACH on the morphology of the resulting DACH-PDA



Scheme 1: The general approach to synthesis of chiral polycatecholamines with the addition of DACH.

particles, the experiment was executed across varying molar ratios of DACH to dopamine, spanning from 2:1 to 0.25:0:1.

Following the well-documented Raper-Mason mechanism, the polymerization commences with the oxidation of dopamine to dopaquinone, which subsequentially undergoes cyclization to yield leucodopaminochrome [45,46]. This intermediate is then transformed into 5,6-dihydroxyindole, constituting the foundational unit of PDA. Concurrently, the nascent PDA oligomers commence agglomeration, culminating in the formation of insoluble particles. The reaction's culmination point is marked by the segregation of two distinct fractions: an insoluble component, amenable to centrifugation and separation, and supernatants enriched with smaller oligomers manifesting as nanoaggregates. The intricate structure of PDA remains a subject of ongoing debate within the scholarly discourse. However, it is acknowledged that the presence of quinone groups within PDA facilitates reactivity with nucleophilic entities, such as amines and thiols, through mechanisms including Schiff base formation and Michael-type addition reactions. In our experimental approach, (R,R)-DACH, which possesses two amino functionalities, was utilized to interlink with those groups, subsequently affecting the growth

of PDA particles during polymerization (Figure 1 and Figure S1). A notable attribute of these particles was their high monodispersity, as quantitatively corroborated by the polydispersity index (PDI) values, ranging from 0.028 to 0.168, as determined *via* DLS measurements (Table S1). These PDI metrics are atypical for PDA particles synthesized *via* alternative methodologies. Moreover, the particles demonstrated high colloidal stability in aqueous environments, as evidenced by their pronouncedly negative zeta potential values.

To dissect the morphology of the residual low-mass oligomer/nanoaggregates dispersed within the solution, a methodology involving drop-casting onto silicon wafers was meticulously applied, succeeded by an examination through SEM. This analytical probe revealed the emergence of distinct "dumpling-like structures." Notably, the morphological attributes, encompassing both dimensions and the degree of uniformity of these structures, were observed to be intricately influenced by the molar ratio of DACH to dopamine employed during the polymerization process. It was discerned that a reduction in the DACH concentration precipitated the formation of "dumplings" that were not only smaller in size but also exhibited a marked increase in uniformity, as visually encapsulated

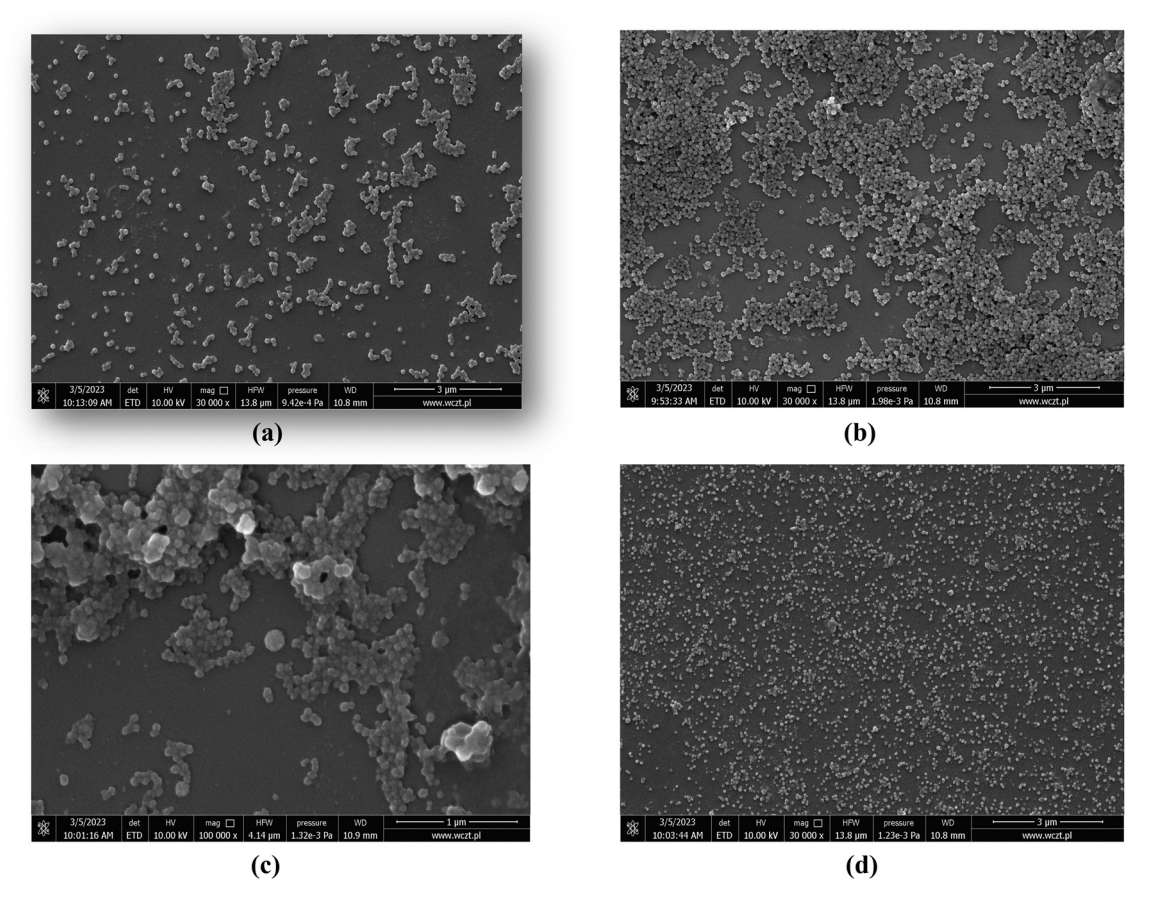


Figure 1: The SEM images of (*R*,*R*)-DACH-PDA particles obtained with different molar ratios of (*R*,*R*)-DACH to dopamine: (a) 2:1, (b) 1:1, (c) 0.5:1, and (d) 0.25:0.1.

in Figure 2, delineating a comparative analysis between panels A and D.

It is imperative to acknowledge the seminal work by Zhang et al., which delineated the formation of PDA nanoaggregates via dopamine polymerization in the milieu of achiral ethylenediamine, facilitating the emergence of fractal patterns on silicon through a dynamic self-assembly mechanism [47]. This assembly is propelled by solvent evaporation, inducing a multidirectional aggregation of particles through the capillary and Marangoni flows, culminating in fractal formations. In the context of our study, while analogous dynamics are conceivable, fractal patterns were not observed. Instead, our investigations unveiled the formation of micrometric "dumpling-like" structures, attributable to the inclusion of (R,R)-DACH during polymerization. The bivalent nature of (R,R)-DACH, featuring two diamine groups, fosters attachment to PDA aggregates at divergent angles relative to the planar configuration and bulkier cyclohexane ring of ethylenediamine. Consequently, the morphologies resulting from dynamic self-assembly in our experiments diverge significantly from those previously reported. To further explore

this phenomenon, a series of experiments were conducted across a pH spectrum of 7.5-9.5 in the TRIS buffer, given the pivotal role of pH in the polymerization and subsequent self-assembly of PDA nanoaggregates (Figure S2). A focused examination on two molar ratios of dopamine to (R,R)-DACH, 1:1 and 0.25:1, revealed pronounced morphological distinctions in the resultant patterns. Scanning electron microscopy (SEM) analysis corroborated that "dumpling-like structures" predominantly emerged at pH values of 9 and 9.5, whereas a reduction in pH favoured the development of ordered filmlike structures, especially pronounced at a (R,R)-DACH:dopamine ratio of 0.25:1. Irrespective of the pH conditions, the formation of spherical and well-dispersed solid particles was observed, with optimal morphology manifesting at elevated pH values. However, particle agglomeration was notably evident at a pH of 7.5 for both examined ratios (Figures S3-S5).

Subsequent investigations aimed to ascertain the impact of substrate character on the self-assembly process. Supernatants derived post-polymerization between (*R,R*)-DACH and dopamine, in ratios of 1:1 and 0.25:1, were drop-casted onto glass

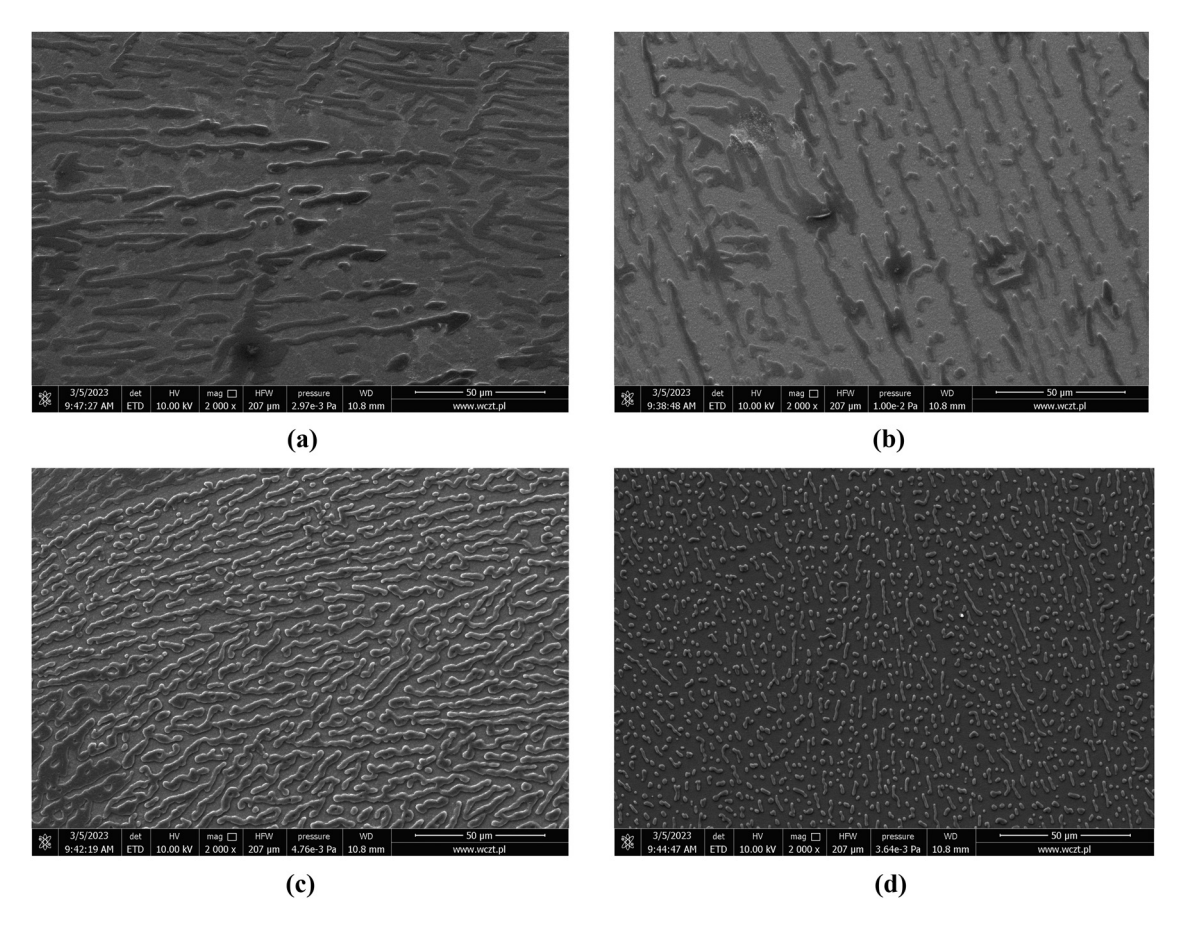


Figure 2: The SEM images of the self-assembled pattern of (*R*,*R*)-DACH-PDA obtained with different molar ratios of (*R*,*R*)-DACH:dopamine: (a) 2:1, (b) 1:1, (c) 0.5:1, and (d) 0.25:1.

and aluminium foil substrates, contrasting in surface chemical composition. SEM analyses revealed that "dumpling-like structures" failed to materialize on these alternative substrates, instead adopting film-like arrangements (Figure S6). This observation underscores the criticality of interactions between nanoaggregates and the substrate in dictating the self-assembly trajectory. Nevertheless, the replacement of silicon wafers with aluminium or glass substrates did not significantly alter the morphology or behaviour of the solid particles yielded from the reaction (Figure S7).

After evaluating the self-assembly process and particle formation in the reaction of (R,R)-DACH and dopamine, we move to the evaluation of their chiral structure by means of CD experiments which also prove the influence of DACH on the structure of obtained polymers. The CD measurements for materials obtained from dopamine polymerization in the presence of (R,R)-DACH were performed on both the supernatant and the particle suspension. Since the concentration of the obtained suspension of particles was low, it was decided to perform further research on supernatant solutions. Because the shape of the CD spectra was the

same in both cases, it was assumed that the spatial structure of the obtained particles is analogous, and the fractions differ only in length and possible cross-linking of the obtained polymer particles (Figure 3a).

In order to estimate the amount of the chiral component involved in the polymerization and built within the structure of DACH-PDA, a number of measurements with different amounts of DACH were performed.

Since PDA is not optically active, the Cotton effects visible in the CD spectrum come only from the change in its structure during polymerization with DACH. Since DACH does not have absorbing chromophores in the tested range, it can be assumed that the spectrum is generated by the mutual arrangement of chromophores present in PDA. A series of measurements with different molar ratios of PDA to DACH showed that the effect of the chiral conformation of PDA molecules begins to be visible in the CD spectrum at a ratio of 0.25:1 and becomes maximal at a ratio of 1:1 (Figure 3b). Increasing the molar ratio to 2:1 did not result in any further increase in Cotton's effects. In order to determine the thermal stability of the obtained material after CD

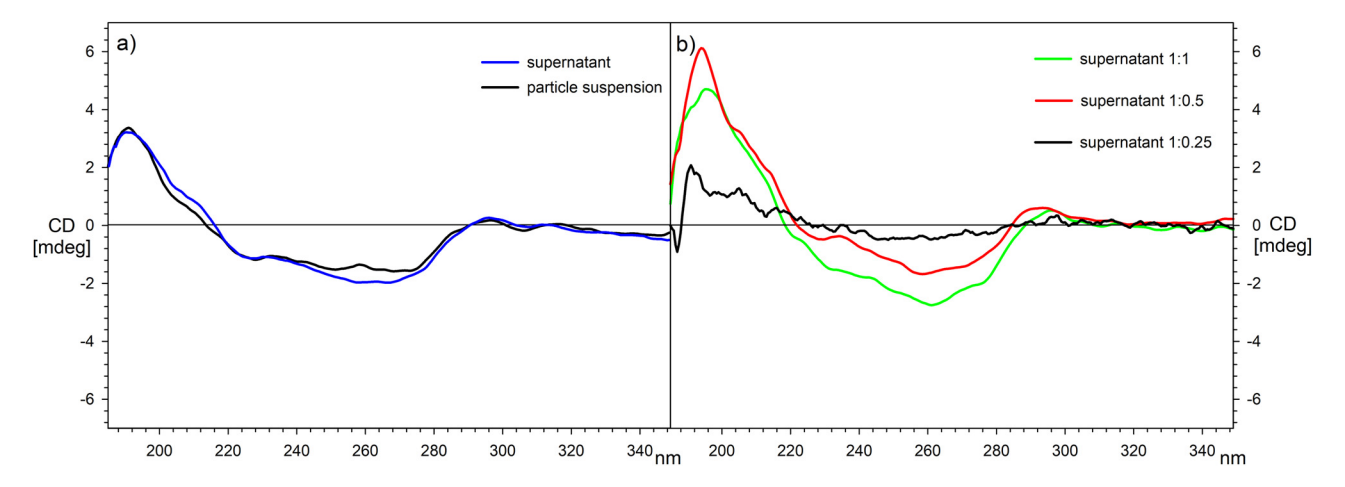


Figure 3: (a) CD spectra of supernatant (blue line) and particles (black line) obtained in the reaction of (*R,R*)-DACH with dopamine at molar ratio 1:1. (b) CD spectra of (*R,R*)-DACH-PDA materials obtained from different molar ratios of dopamine to DACH.

measurements, the same sample obtained in the reaction (*R*,*R*)-DACH:dopamine at the ratio 1:1 was incubated at 80°C for 2 h. No changes in the CD spectra indicate that the chiral structure of the molecules is thermally stable. The CD spectra of the material suspension before and after incubation are shown in Figure 4a. Due to the structure of the substrates used for polymerization, the question arose whether they are resistant to acids. In this case, there may be both protonation of the amino groups and hydrolysis of the imines that may have resulted from the reaction to form the material. Since protonation of amines occurs almost instantaneously and hydrolysis of imines is slower, CD spectra of the material were measured immediately after protonation and after 2 h. and it was proven that it is not dependent on the protonation of amino groups (Figure 4b).

3.2 Path B – reaction of L-DOPA with chiral 1,2-diaminocyclohexane

In the subsequent phase of our research, we decided to employ L-DOPA, a naturally occurring precursor for the synthesis of melanin, as a means to generate adhesive coatings and particles for various applications through oxidative polymerization, similar to dopamine. The structure of the resulting PLDOPA remains unidentified, displaying a comparable level of heterogeneity to PDA. The initial stages of polymerization may also adhere to the Raper–Mason mechanisms observed in PDA. Unlike dopamine, PLDOPA possesses a stereogenic centre that could potentially influence the behaviour of molecular self-assembly. Furthermore, L-DOPA, being an amino acid, may exhibit distinct interactions

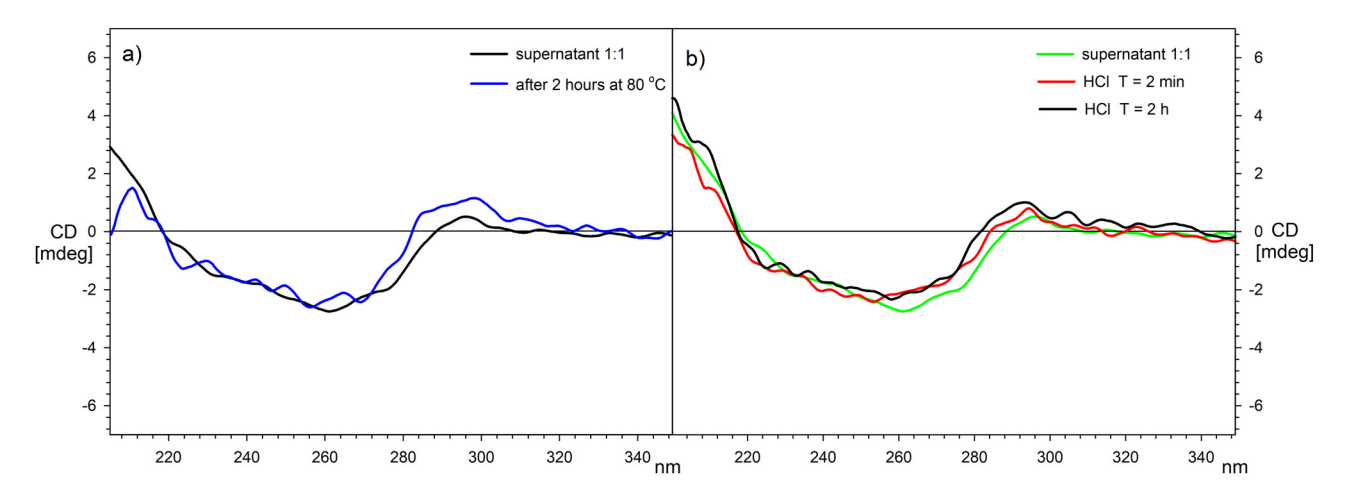


Figure 4: (a) CD spectra of the material (*R*,*R*)-DACH-PDA after protonation with 2M HCL after 2 min and 2 h. (b) The same sample after protonation with 2 M HCl after 2 min and 2 h.

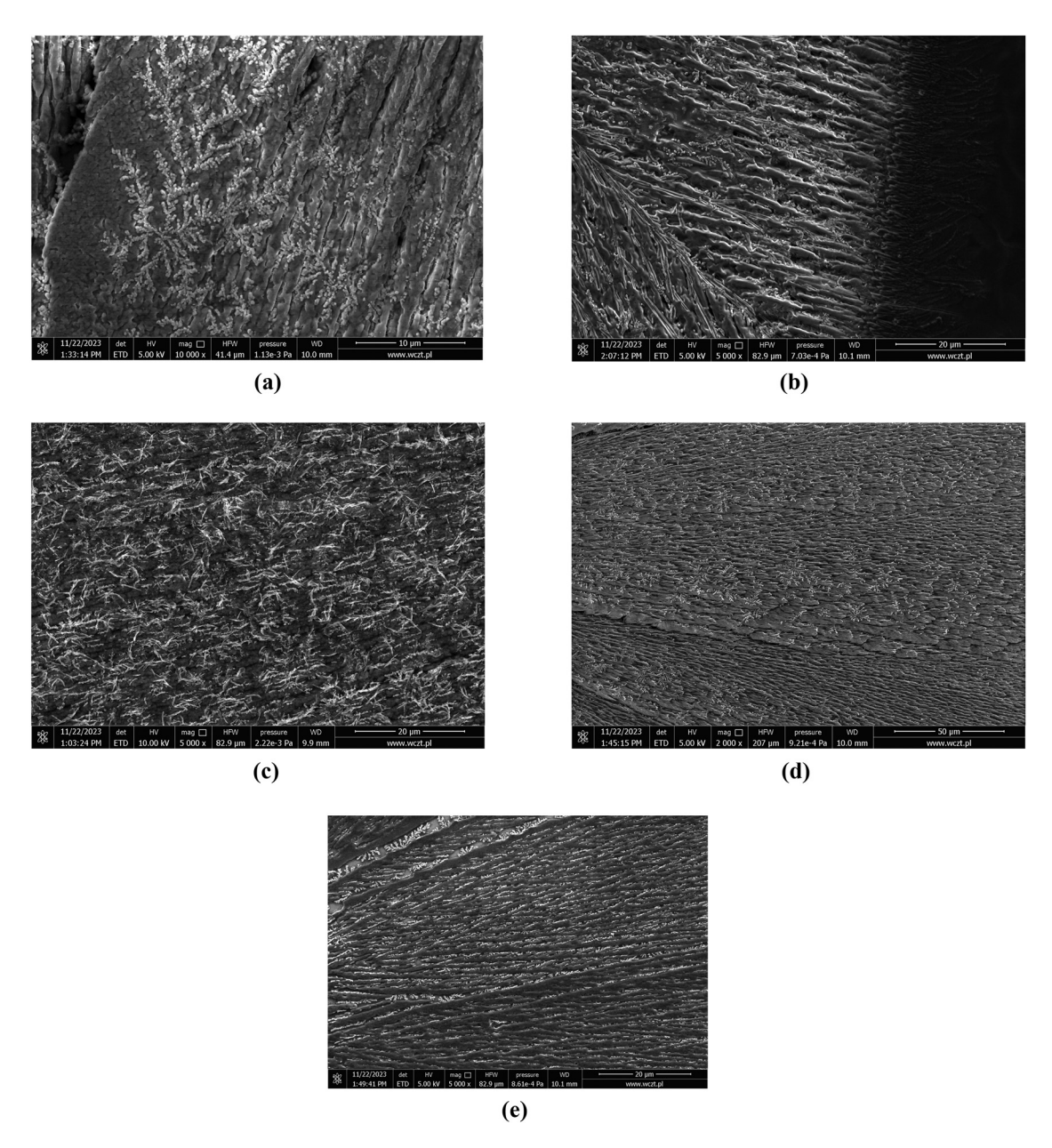


Figure 5: The SEM images of the self-assembled pattern of (*R*,*R*)-DACH-PLDOPA particles obtained with different ratios of DACH to L-DOPA: (a) 2:1, (b) 1:1, (c) 0.5:1, (d) 0.25:1, and (e) only PLDOPA.

with DACH due to the presence of a carboxylic group, thereby influencing the formation of surface patterns. Ultimately, we hypothesized that the reaction with different DACH enantiomers could yield different diastereomeric products, consequently altering the self-assembly process and resulting in variations in morphology and patterns. Our preliminary experiment involved the reaction of L-DOPA with (R,R)-DACH under conditions similar to those used for dopamine while maintaining an L-DOPA concentration of 1 × 10⁻³ mol. After 24 h, solid particles could not be separated from the mixture even at a speed of 14,000 rpm, indicating the presence

of stable oligomers/nanoaggregates. As a result, we directly applied the sample onto a silicon support.

The morphology of the structures obtained is illustrated in Figure 5. The alteration of the substrate in the reaction seems to have an impact on their morphology, as the formation of the "microdumpling" structure was not observed. Instead, a dense fibrous carpet was formed. Interestingly, similar carpet formations were also observed with L-DOPA, indicating that the influence of (*R*,*R*)-DACH on the resulting patterns may not be as significant as in dopamine polymerization. We hypothesized that the

interactions between (R,R)-DACH and PLDOPA nanoaggregates and their arrangement play a crucial role in the formation of these patterns. To determine the size of nanoaggregates/particles in the reaction mixture, DLS analysis was conducted. The analysis revealed a significant variation in particle sizes, with a PDI index above 0.3, indicating polydispersity in terms of particle size for all tested DACH:L-Dopa ratios as well as for pure PLDOPA (Table S2). This diversity in particle sizes affects the self-assembly process during sample evaporation, thereby influencing the resulting patterns. The wide range of particle sizes observed may be attributed to the heterogeneous integration of DACH molecules within the nanoaggregates/nanoparticles formed during the polymerization process. This, in turn, leads to the development of different fractions of particles that contribute to the production of PLDOPA. Furthermore, it is important to consider the potential influence of the intrinsic properties of L-DOPA during the polymerization process.

The current approach also involved an examination of particle size after the polymerization process using DLS, similar to previous experiments. The results obtained from our experiments displayed the behaviour of nanoaggregates and particles gained from the polymerization process akin to previous findings, leading to the generation of highly polydispersed samples (Table S2). This outcome suggests that a wide array of nanostructures contributed to the formation of patterns on the surfaces post-polymerization. Interestingly, the morphology observed in this study differs from that observed when DACH was utilized, indicating that distinct diastereoisomeric pairs influenced the supramolecular arrangement of molecules during dynamic self-assembly processes, resulting in diverse structural patterns.

In our subsequent approach to comprehending the impact of DACH on the self-assembly process of PLDOPA, we employed (*S*,*S*)-DACH instead of (*R*,*R*)-DACH. By doping chiral L-DOPA or chiral PLDOPA nanoaggregates with this compound, we anticipated the formation of diastereomeric structures distinct from those formed in the case of (*R*,*R*)-DACH. We have assumed that this change in structure could potentially have implications for the self-assembly process and the generation of intermediates. Notably, the SEM analysis of the resulting patterns from the reaction between these two molecules revealed the emergence of structures resembling "dumplings" similar to those observed

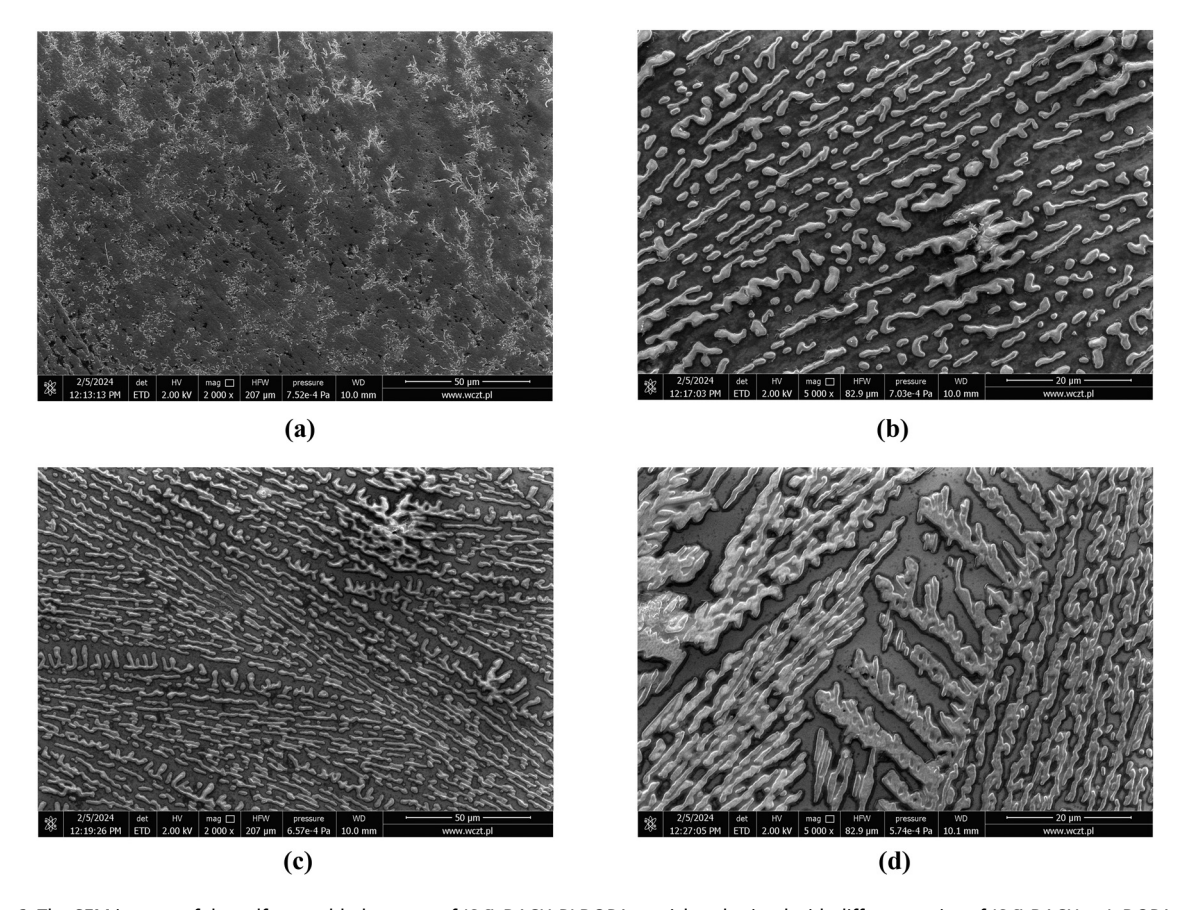


Figure 6: The SEM images of the self-assembled pattern of (*S*,*S*)-DACH-PLDOPA particles obtained with different ratios of (*S*,*S*) DACH to L-DOPA: (a) 2:1, (b) 1:1, (c) 0.5:1, and (d) 0.25:1.

in the reaction involving DACH and dopamine rather than curly carpets recorded in the reaction of L-DOPA with (R,R)-DACH. The morphology of these obtained structures is visually depicted in Figure 6.

In light of the morphological variations observed in the polymerization products of L-DOPA with enantiopure forms of DACH, namely, (R,R)-DACH and (S,S)-DACH, we move to CD experiments to assess differences in absorption of polarized light by these polymers. Our objective was to ascertain whether the distinct interaction mechanisms between (R,R)-DACH and (S,S)-DACH with PLDOPA can be elucidated through their optical activity. This investigation was performed to provide insights into the phenomenon of pattern diversification manifested through self-assembly processes. By analysing the optical spectra of the resulting polymers, we aimed to reveal the underlying stereochemical influences that govern their structural and morphological characteristics. In the case of measuring a polymer based on L-DOPA and DACH, it should be taken into account that L-DOPA is chiral itself and its polymer generates Cotton effects in the CD spectrum. Therefore, it is necessary to refer the spectra of polymers with DACH additives to the spectrum of the L-DOPA polymer obtained under the same conditions and the same concentration. The CD spectrum of PLDOPA shows a negative effect of -4.86 mdeg with a maximum located at 278 nm and a positive effect of 3.00 mdeg with a maximum at 223 nm. In order to determine the possible types of diastereomeric interactions during polymerization and their impact on conformations of products, a series of measurements were performed for both DACH enantiomers and additionally for DACH in the racemic form.

The polymer obtained from L-DOPA and (R,R)-DACH showed different properties than PDAs obtained in reactions with (R,R)-DACH. In this case, notable changes in the CD spectra can only be observed at a molar ratio of L-DOPA to (R,R)-DACH 1:1 and more. This is manifested by the disappearance of the negative Cotton effect at 278 nm from -4.56 mdeg down to -1.48 mdeg at 2:1 L-DOPA to (R,R)-DACH molar ratio and decay of the Cotton effect at 222 nm from 3.00 mdeg to 1.45 mdeg. These changes are connected with the emergence of a new positive Cotton effect up to 2.68 mdeg at approximately 310 nm and negative -1.59 mdeg at around 378 nm This effect may be related to the formation of chiral structures with a delocalized system of π electrons of lower transition energy.

Since diastereomeric interactions occur in the reaction system in which both copolymerizing components are chiral, it was necessary to investigate the polymerization reaction of L-DOPA with the second enantiomer (*S,S*)-DACH. The results of CD measurements indicate a more noticeable

decrease in the Cotton effect located round 278 nm up to the 4.41 mdeg for the 1:2 ratio as well as a very strong change in the short-wave effect located at approximately 200 nm amounting to -8.20 mdeg for 198 nm. In the case of polymerization with the (S,S)-DACH enantiomer, changes in the CD spectra are visible even from a small addition of (S,S)-DACH (DACH:L-DOPA ratio 0.25:1). Both of these changes indicate differences related to the arrangement of L-DOPA fragments in the material. The main difference, however, is the lack of long-wavelength effects at 310 and 370 nm observed for the material obtained in the polymerization of L-DOPA with (R.R)-DACH. These results indicate that not only are the DACH fragments interconnected in the material, but also that no new structures containing long-wavelength transitions are formed as a result of polymerization. Therefore, the observed behaviour of materials in CD measurements proved the different roles of each DACH enantiomer in the polymerization process and its impact was reflected by deferent morphology of obtained patterns via self-assembly.

Since the UV spectrum is influenced not only by the absorption of the tested material but also by scattering of nanoparticles, it is not unequivocal in interpretation, but it can be seen that in the UV spectrum of the material made from L-DOPA and (*R*,*R*)-DACH, there is a UV maximum of low intensity located at 343 nm, while no such maximum is visible for the polymer based on (*S*,*S*)-DACH. This additionally suggests that during polymerization with (*S*,*S*)-DACH, structures generating such electronic transitions are not formed.

The CD spectra of a polymer based on L-DOPA and racemic *rac*-DACH in the short-wavelength regions change as can be expected on the basis of the observations of CD spectra of materials obtained from L-DOPA and pure enantiomers of DACH and PDA. In the long-term spectra above 300 nm, changes are much smaller than expected, which indicates that the presence of (*S,S*)-DACH influences negatively the formation of structures with a high degree of double bond conjugation. A comparison of the CD spectra of L-DOPA and DACH is shown in Figure 7(a)–(c).

3.3 Path C – doping racemic D/L norepinephrine with chiral DACH

In our approach to understand the role of DACH as a dopant and its interaction with catecholamines, we chose D/L-norepinephrine, which possesses a stereogenic centre but is racemic. By employing such a molecule, we aimed to observe how chiral (R,R)-DACH influences the material

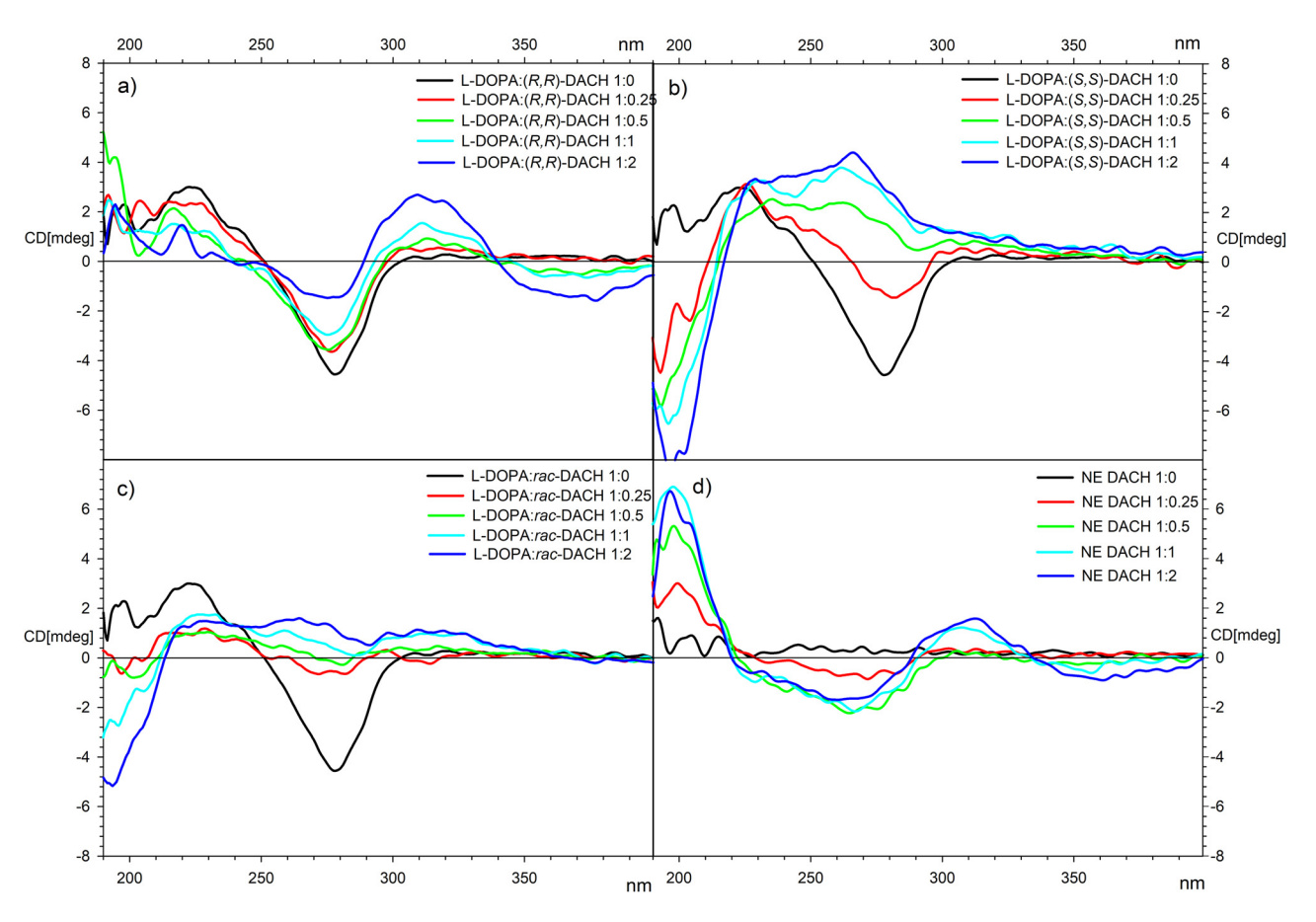


Figure 7: CD spectra recorded for materials obtained in the reaction between (a) L-DOPA-(*R*,*R*)-DACH, (b) L-DOPA-(*S*,*S*)-DACH, (c) L-DOPA-*rac*-DACH, and (d) D/L – norepinephrine and (*R*,*R*)-DACH.

properties, particularly its preferential interaction with one enantiomer of catecholamines. Unlike the case with L-DOPA, the formation of particles was observed here, and they could be separated from the reaction mixture by centrifugation. The morphology of the particles is shown in the Figure S8 in the Supplementary Information (SI). The DLS measurements revealed that the particle/nanoaggregates present in the reaction mixture varied in size from 55 to 160 nm, as determined by DLS measurements. Moreover, we observed that the impact of (R,R)-DACH on particle size was significant since at the ratio of 2:1 DACH to D/L-norepinephrine, the particles exhibited a size of 55 nm with a PDI of 0.087, indicating a rather narrow distribution. However, with a decreasing concentration of (R,R)-DACH, we recorded that the PDI index of the particles increased, and the particle size grew larger, reaching 160 nm at a ratio of 0.25:1, with a PDI index of 0.430 (Table S3). It is worth highlighting that the particle charge became more negative with the decrease in DACH concentration, shifting from -20 to -33 mV. This change suggests an increase in the number of catechol groups that could undergo deprotonation in basic connections, indirectly

proving that DACH was incorporated into the structure of the resulting polymers.

As in previous cases, the self-assembly patterns were visualized by SEM and are depicted in Figure 8. It is evident that with a decreasing amount of DACH in the reaction, the surface pattern changes. At the ratio of 2:1 DACH to D/Lnorepinephrine, we observed a fragmented film that formed a kind of "island." The morphological distinctions of the structures derived from the polymerization of dopamine and L-DOPA, as compared to those obtained from reactions involving chiral DACH and D/L -norepinephrine, suggest a multifaceted influence on the polymer formation process. It is evident that the nature of the chiral DACH is a critical factor; however, the unique structural configurations and stereochemical properties of the catecholamines themselves also play a significant role in dictating the characteristics of the resultant polymers. A further decrease in DACH concentration in the polymerization reaction resulted in a more ordered structure, which appears to be quite sensitive.

CD studies on DACH-PNOR obtained in the reaction of *rac*-norepinephrine and (*R*,*R*)-DACH indicated the formation

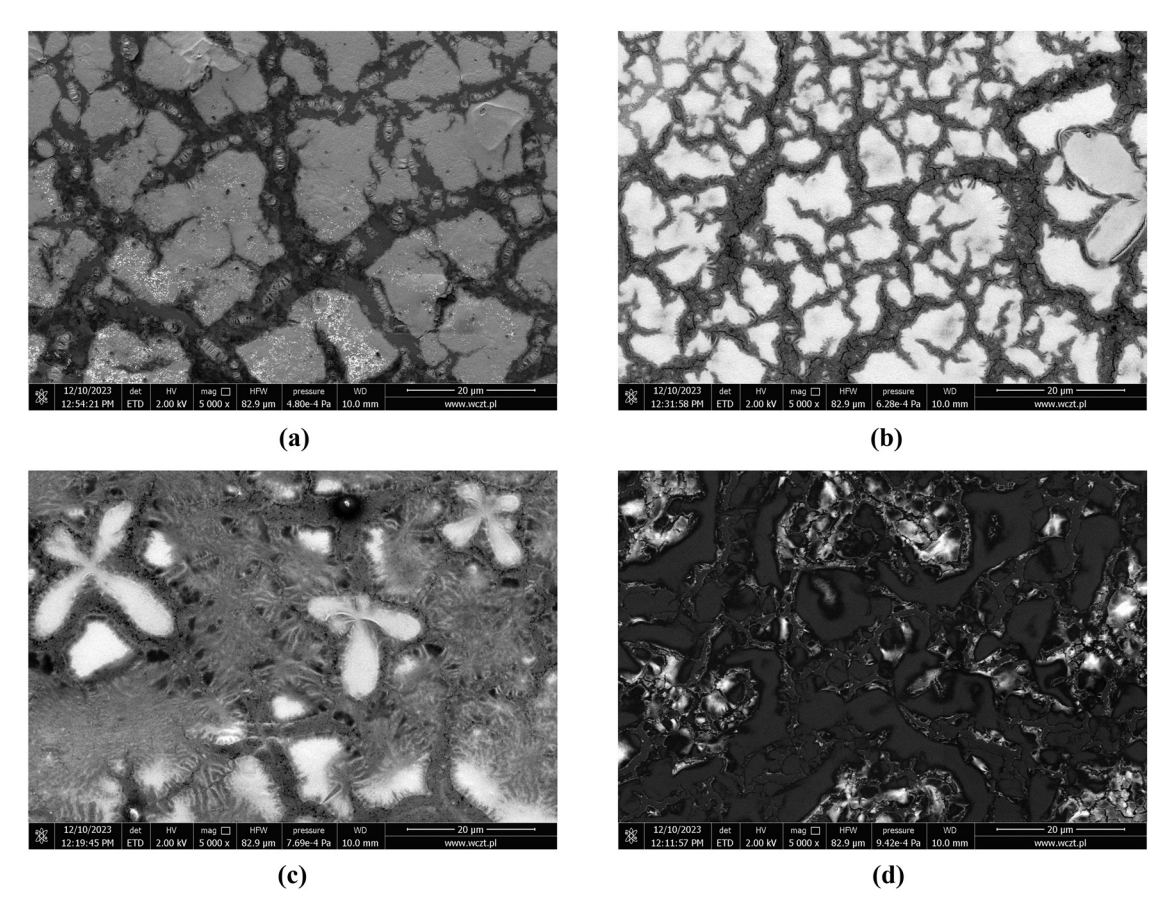


Figure 8: The SEM images of the self-assembled pattern of (R,R)-DACH-PNOR particles obtained with different ratios of (R,R)-DACH to D/L-Norepinephrine ratio: (a) 2:1, (b) 1:1, (c) 0.5:0.1, and (d) 0.25:1.

of chiral arrangements of chromophores in the resulting polymer. In the short-wavelength range below 300 nm, the formation of a negative Cotton effect with a maximum at 266 nm and a positive Cotton effect at 198 nm can be observed. Their increase can be observed already from the addition of 25 mol% (R,R)-DACH, and the maximum values of -1.73 mdeg at 266 nm and 6.93 mdeg at 198 were obtained already for the addition of 50 mol% (R,R)-DACH. A further increase in the amount of DACH in the mixture does not result in further changes in the CD spectra in this range. In the long-term spectral range, above 300 nm, Cotton Effects can be observed only with the equimolar or larger addition of (R,R)-DACH. The maxima are located at 312 nm (1.58 mdeg) and 362 nm (-0.95 mdeg) for the 2 equimolar (R,R)-DACH addition. This situation is analogous to that observed for the polymerization of L-DOPA with (R,R)-DACH and may indicate that in this case also structures with lower electronic transition energy are formed. The spectra of rac-norepinephrine from (R,R)-DACH are shown in Figure 7d.

Since no long-term Cotton effects were observed above 300 nm for materials based on PDA, it can be assumed that the chirality element in the side chain of the catechol used

is the key to their formation. The measurement results additionally indicate that only some diastereomeric interactions lead to the formation of structures exhibiting Cotton effects above 300 nm. This opens a new path for research on chiral polycatechol materials with a precisely defined structure caused by structural modifications of polycatechol monomers.

The summary of maxima of Cotton effects due to used catecholamine to DACH molar ratio changes for all discussed cases are presented in Tables S4–S6 in SI.

4 Conclusion

In conclusion, we propose a new approach towards chirality induction in polycatecholamine polymers, synthesized from dopamine, L-DOPA, and D/L-norepinephrine, through the incorporation of optically active DACH into the polymerization process. The addition of DACH significantly influences both the formation of polymer particles and their stability in solution as well as their size in case of

dopamine polymerization. Moreover, the oligomers/nanoaggregates remaining in the polymerization solution undergo self-assembly on silicon wafers, forming unique structures that have been not observed before. CD analysis of materials, synthesized by adding either (R,R)- or (S,S)-DACH to the polymerization of L-DOPA, revealed the formation of diastereomers, impacting both the morphology of the selfassembled patterns and aligning with the observations from SEM investigations.

Acknowledgments: The authors are grateful to prof. Emerson Coy form the NanoBioMedical Centre for TEM pictures.

Funding information: R.M is grateful to National Sciences Centre for financial support under the project number UMO-2018/31/B/ST8/02460. H.O.A is thankful to Study@research programme financed from IDUB under project number 134/34/ ID-UB/0019.

Author contributions: H.O.A.: methodology, validation, investigation, writing - review and editing, and engaged in conceptualization; M.W.: methodology, validation, and investigation; J.G.: methodology, validation, investigation, writing - review and editing, and formal analysis; and R.M.: conceptualization, methodology, validation, investigation, writing – original draft, writing – review and editing, visualization, supervision, funding acquisition, resources, and project administration. All authors have accepted responsibility for the entire content of this manuscript and approved its submission.

Conflict of interest: The authors state no conflict of interest.

References

- Dajek M, Kowalczyk R, Boratyński PJ. Trans-1,2-Diaminocyclohexane-based sulfonamides as effective hydrogenbonding organocatalysts for asymmetric Michael-hemiacetalization reaction. Catal Sci Technol. 2018;8:4358-63. doi: 10.1039/C8CY01199K.
- Bennani YL, Hanessian S. Trans-1,2-Diaminocyclohexane derivatives [2] as chiral reagents, scaffolds, and ligands for catalysis: applications in asymmetric synthesis and molecular recognition. Chem Rev. 1997;97:3161-96. doi: 10.1021/cr9407577.
- van Beek C, Samoshin VV. Conformationally locked cis-1,2-diaminocyclohexane-based chiral ligands for asymmetric catalysis. Tetrahedron Lett. 2022;102:153930. https://www.sciencedirect. com/science/article/pii/S0040403922003628.
- Kwit M, Grajewski J, Skowronek P, Zgorzelak M, Gawroński J. Onestep construction of the shape persistent, chiral but symmetrical

- polyimine macrocycles. Chem Rec. 2019;19:213-37. doi: 10.1002/tcr. 201800052.
- Gawroński J, Kwit M, Rychlewska U. 3.11 Trianglamines and related [5] chiral macrocycles. In: Atwood JL, editor. Comprehensive supramolecular chemistry II. Oxford: Elsevier; 2017. p. 267-91. https:// www.sciencedirect.com/science/article/pii/B9780124095472125211.
- Zgorzelak M, Grajewski J, Gawroński J, Kwit M. Solvent-assisted synthesis of a shape-persistent chiral polyaza gigantocycle characterized by a very large internal cavity and extraordinarily high amplitude of the ECD exciton couplet. Chem Commun. 2019;55:2301-4. doi: 10.1039/C8CC10184A.
- He T, Li J, Li X, Ren C, Luo Y, Zhao F, et al. Spectroscopic studies of chiral perovskite nanocrystals. Appl Phys Lett. 2017;111:151102. doi: 10.1063/1.5001151.
- Gao G, Zhang X, Meng D, Zhang A, Liu Y, Jiang W, et al. Bis(perylene diimide) with DACH bridge as non-fullerene electron acceptor for organic solar cells. RSC Adv. 2016;6:14027-33. doi: 10.1039/ C5RA26777C.
- Eaby AC, Myburgh DC, Kosimov A, Kwit M, Esterhuysen C, Janiak AM, et al. Dehydration of a crystal hydrate at subglacial temperatures. Nature. 2023;616:288-92. doi: 10.1038/s41586-023-05749-7.
- [10] Ryu JH, Messersmith PB, Lee H. Polydopamine surface chemistry: a decade of discovery. ACS Appl Mater Interfaces. 2018;10:7523-40. doi: 10.1021/acsami.7b19865.
- Alfieri ML, Weil T, Ng DYW, Ball V. Polydopamine at biological interfaces. Adv Colloid Interface Sci. 2022;305:102689. https:// www.sciencedirect.com/science/article/pii/S0001868622000914.
- Ball V, Hirtzel J, Leks G, Frisch B, Talon I. Experimental methods to [12] get polydopamine films: a comparative review on the synthesis methods, the films' composition and properties. Macromol Rapid Commun. 2023;44:2200946. doi: 10.1002/marc.202200946.
- Baldoneschi V, Palladino P, Scarano S, Minunni M. Polynorepinephrine: state-of-the-art and perspective applications in biosensing and molecular recognition. Anal Bioanal Chem. 2020;412:5945-54. doi: 10.1007/s00216-020-02578-9.
- [14] Tan X, Gao P, Li Y, Qi P, Liu J, Shen R, et al. Poly-dopamine, polylevodopa, and poly-norepinephrine coatings: Comparison of physico-chemical and biological properties with focus on the application for blood-contacting devices. Bioact Mater. 2021;6:285-96. https://www.sciencedirect.com/science/article/pii/ S2452199X20301274.
- [15] Lee H, Dellatore SM, Miller WM, Messersmith PB. Mussel-inspired surface chemistry for multifunctional coatings. Science (1979). 2007;318(5849):426-30.
- Aguilar-Ferrer D, Vasileiadis T, Iatsunskyi I, Ziółek M, Żebrowska K, Ivashchenko O, et al. Understanding the photothermal and photocatalytic mechanism of polydopamine coated gold nanorods. Adv Funct Mater. 2023;33:2304208. doi: 10.1002/adfm. 202304208.
- Szewczyk J, Pochylski M, Szutkowski K, Kempiński M, [17] Mrówczyński R, Iatsunskyi I, et al. In-situ thickness control of centimetre-scale 2D-Like polydopamine films with large scalability. Mater Today Chem. 2022;24:100935. https://www.sciencedirect. com/science/article/pii/S2468519422001641.
- Aguilar-Ferrer D, Szewczyk J, Coy E. Recent developments in polydopamine-based photocatalytic nanocomposites for energy production: Physico-chemical properties and perspectives. Catal Today. 2022;397-399:316-49. https://www.sciencedirect.com/ science/article/pii/S0920586121003722.

- [19] Szewczyk J, Ziółek M, Siuzdak K, Iatsunskyi I, Pochylski M, Aguilar-Ferrer D, et al. Ex-situ transferring of polydopamine films on semiconductor interface: Evidence of functional hybrid heterojunction. Eur Polym J. 2024;206:112781. https://www.sciencedirect.com/science/article/pii/S0014305724000429.
- [20] Coy E, Iatsunskyi I, Colmenares JC, Kim Y, Mrówczyński R. Polydopamine films with 2D-like layered structure and high mechanical resilience. ACS Appl Mater Interfaces. 2021;13:23113–20. doi: 10.1021/acsami.1c02483.
- [21] Liebscher J, Mrówczyński R, Scheidt HA, Filip C, Haidade ND, Turcu R, et al. Structure of polydopamine: A never-ending story? Langmuir. 2013;29:10539–48.
- [22] Mrówczyński R, Magerusan L, Turcu R, Liebscher J. Diazo transfer at polydopamine-a new way to functionalization. Polym Chem. 2014;5:6593–9.
- [23] Szukowska M, Popenda Ł, Coy E, Filip C, Grajewski J, Kempiński M, et al. Replacing amine by azide: dopamine azide polymerization triggered by sodium periodate. Polym Chem. 2022;13:3325–34. doi: 10.1039/D2PY00293K.
- [24] Gu GE, Park CS, Cho H-J, Ha TH, Bae J, Kwon OS, et al. Fluorescent polydopamine nanoparticles as a probe for zebrafish sensory hair cells targeted in vivo imaging. Sci Rep. 2018;8:4393. doi: 10.1038/ s41598-018-22828-2.
- [25] Barclay TG, Hegab HM, Clarke SR, Ginic-Markovic M. Versatile surface modification using polydopamine and related polycatecholamines: chemistry, structure, and applications. Adv Mater Interfaces. 2017;4:1601192. doi: 10.1002/admi.201601192.
- [26] Li C, Yang Q, Chen D, Zhu H, Chen J, Liu R, et al. Polyethyleneimineassisted co-deposition of polydopamine coating with enhanced stability and efficient secondary modification. RSC Adv. 2022;12:35051–63. doi: 10.1039/D2RA05130C.
- [27] Huang T, Cao S, Luo D, Zhang N, Lei Y, Wang Y. Polydopamineassisted polyethylenimine grafting melamine foam and the application in wastewater purification. Chemosphere. 2022;287:132054. https://www.sciencedirect.com/science/article/pii/ S0045653521025261.
- [28] Lv Y, Yang S-J, Du Y, Yang H-C, Xu Z-K. Co-deposition kinetics of polydopamine/polyethyleneimine coatings: effects of solution composition and substrate surface. Langmuir. 2018;34:13123–31. doi: 10.1021/acs.langmuir.8b02454.
- [29] Mrówczyński R, Grześkowiak BF. Biomimetic catechol-based nanomaterials for combined anticancer therapies. Nanoengineering of biomaterials: biomedical applications, II. Weinheim, Germany: WILEY-VCH GmbH; 2022. p. 145–80.
- [30] Grześkowiak BF, Maziukiewicz D, Kozłowska A, Kertmen A, Coy E, Mrówczyński R. Polyamidoamine dendrimers decorated multifunctional polydopamine nanoparticles for targeted chemo- and photothermal therapy of liver cancer model. Int J Mol Sci. 2021;22:145–80. https://www.mdpi.com/1422-0067/22/2/738.
- [31] Mrówczyński R. Polydopamine-based multifunctional (Nano)materials for cancer therapy. ACS Appl Mater Interfaces. 2018;10:7541–61. doi: 10.1021/acsami.7b08392.
- [32] Lu Z, Douek AM, Rozario AM, Tabor RF, Kaslin J, Follink B, et al. Bioinspired polynorepinephrine nanoparticles as an efficient

- vehicle for enhanced drug delivery. J Mater Chem B. 2020;8:961–8. doi: 10.1039/C9TB02375E.
- [33] Michalicha A, Roguska A, Przekora A, Budzyńska B, Belcarz A. Poly (levodopa)-modified β-glucan as a candidate for wound dressings. Carbohydr Polym. 2021;272:118485. https://www.sciencedirect. com/science/article/pii/S0144861721008729.
- [34] Lu Z, Teo BM, Tabor RF. Recent developments in polynorepinephrine: an innovative material for bioinspired coatings and colloids. J Mater Chem B. 2022;10:7895–904. doi: 10.1039/D2TB01335E.
- [35] Lu Z, Quek AJ, Meaney SP, Tabor RF, Follink B, Teo BM. Polynorepinephrine as an efficient antifouling-coating material and its application as a bacterial killing photothermal agent. ACS Appl Bio Mater. 2020;3:5880–6. doi: 10.1021/acsabm.0c00578.
- [36] Hao C, Wang G, Chen C, Xu J, Xu C, Kuang H, et al. Circularly polarized light-enabled chiral nanomaterials: from fabrication to application. Nanomicro Lett. 2023;15:39. doi: 10.1007/s40820-022-01005-1.
- [37] Fu W, Tan L, Wang P. Chiral inorganic nanomaterials for photo (electro)catalytic conversion. ACS Nano. 2023;17:16326–47. doi: 10. 1021/acsnano.3c04337.
- [38] Kwon J, Choi WJ, Jeong U, Jung W, Hwang I, Park KH, et al. Recent advances in chiral nanomaterials with unique electric and magnetic properties. Nano Converg. 2022;9:32. doi: 10.1186/s40580-022-00322-w.
- [39] Yang Z, Jaiswal A, Yin Q, Lin X, Liu L, Li J, et al. Chiral nanomaterials in tissue engineering. Nanoscale. 2024;16:5014–41. doi: 10.1039/ D3NR05003C.
- [40] Wang G, Zhang H, Kuang H, Xu C, Xu L. Chiral inorganic nanomaterials for bioapplications. Matter. 2023;6:1752–81. https://www. sciencedirect.com/science/article/pii/S2590238523001686.
- [41] Bartolomei B, Corti V, Prato M. Chiral carbon nanodots can act as molecular catalysts in chemical and photochemical reactions. Angew Chem Int Ed. 2023;62:e202305460. doi: 10.1002/anie. 202305460.
- [42] Đorđević L, Arcudi F, D'Urso A, Cacioppo M, Micali N, Bürgi T, et al. Design principles of chiral carbon nanodots help convey chirality from molecular to nanoscale level. Nat Commun. 2018;9:3442. doi: 10.1038/s41467-018-05561-2.
- [43] Maniappan S, Reddy KL, Kumar J. Transmitting biomolecular chirality into carbon nanodots: a facile approach to acquire chiral light emission at the nanoscale. Chem Sci. 2023;14:491–8. doi: 10.1039/D2SC05794H.
- [44] Awasthi AK, Bhagat SD, Ramakrishnan R, Srivastava A. Chirally twisted ultrathin polydopamine nanoribbons: synthesis and spontaneous assembly of silver nanoparticles on them. Chem – A Eur J. 2019;25:12905–10. doi: 10.1002/chem.201902600.
- [45] Mason HS. The chemistry of melanin: III. Mechanism of the oxidation of dihydroxyphenylalanine by tyrosinase. J Biol Chem. 1948;172:83–99. https://www.sciencedirect.com/science/article/pii/S002192581835614X.
- [46] Raper HS. The aerobic oxidases. Physiol Rev. 1928;8:245–82. doi: 10.1152/physrev.1928.8.2.245.
- [47] Zhang P, Tang A, Zhu B, Zhu L, Zeng H. Hierarchical self-assembly of dopamine into patterned structures. Adv Mater Interfaces. 2017;4:1601218. doi: 10.1002/admi.201601218.